Journal of Materials Chemistry B



PAPER

View Article Online
View Journal | View Issue

Plasmonic liposomes for synergistic photodynamic and photothermal therapy†

Cite this: J. Mater. Chem. B, 2014, 2, 2592

Jeongmin Oh, ‡a Hwan-Jun Yoon ‡a and Ji-Ho Park*ab

In the present study, plasmonic liposomes (PLs) loaded with photosensitizers were developed for synergistic photodynamic and photothermal therapy. These PLs were prepared by incorporating a photosensitizer, ZnPc, into the liposomal membrane for photodynamic therapy (PDT) and coating a gold nanofilm onto the surface for photothermal therapy (PTT). The gold coating was optimized to efficiently absorb the wavelength of light at which ZnPc is activated for PDT. The photosensitizing effect of ZnPc was synergistically enhanced upon single light irradiation due to local photothermal heating and the surface plasmon resonance of the gold nanostructure. Furthermore, combined photodynamic and photothermal therapy using ZnPc-PLs exhibited a remarkably enhanced therapeutic efficacy on cancer cells *in vitro* compared to PDT or PTT alone. Therefore, we believe that this dual photoactive nanodevice with a synergistic therapeutic index has great potential to improve the current phototherapy of cancer.

Received 16th October 2013 Accepted 7th January 2014

DOI: 10.1039/c3tb21452d www.rsc.org/MaterialsB

1. Introduction

Phototherapy is a well established treatment for many diseases, including cancer, due to the selective and localized therapeutic effect caused by laser irradiation.1-3 Far-red (FR) and nearinfrared (NIR) light in range of 650-900 nm have been preferable for phototherapy over ultraviolet (UV) and visible light due to their low phototoxicity and high tissue penetration. There are two major types of phototherapy: photodynamic therapy (PDT) and photothermal therapy (PTT). PDT, a non-invasive therapy currently used in clinics, uses photosensitizers that generate cytotoxic singlet oxygen upon laser irradiation. Zinc phthalocyanine (ZnPc) has been suggested as a promising photosensitizer due to its high phototoxicity in the FR-NIR region.^{4,5} However, ZnPc is prone to aggregation under physiological conditions due to its hydrophobicity, which significantly reduces its photosensitizing effect. In order to improve its low solubility, many amphiphilic nanocarriers have been developed that incorporate ZnPc into their internal hydrophobic space.⁶⁻⁹ Among such nanocarriers, clinically-approved liposomes are the most promising, because they allow for efficient loading of monomeric ZnPc molecules into their transmembranes, and selective delivery to target sites. The monomeric form of ZnPc has been known to improve its photosensitizing efficiency and

PTT damages malignant cells with heat converted from light by photoactive agents. A variety of gold nanoparticles including nanoshells, nanocages, and nanorods have been extensively investigated as potential PTT agents because they show excellent biocompatability and high photothermal conversion efficiency for wavelengths at which tissues are relatively transparent. The structure is the main factor determining the absorption wavelengths of gold nanoparticles. However, PTT requires a relatively high temperature (>60 °C) to destroy cancer cells. Such intense heating would cause unintended damage to surrounding normal tissues, reducing the potential of its clinical translation.

Due to the limitations shown by singular treatments, there has been increasing interest in combining PDT and PTT by incorporating photosensitizers into single nanoparticle platforms. 18-33 However, most of these efforts could not be photoactivated with a single light source due to the difference between the light absorption wavelengths of the nanomaterial and photosensitizer.20-23,28,29,32,33 By matching the absorption wavelength of the inorganic nanomaterial with the excitation wavelength of photosensitizer, simultaneous PDT and PTT, upon single-laser irradiation, were also performed for some of these nanosystems. 18,19,26,27,30,31 Although these combined phototherapies exhibited superior therapeutic outcomes compared to singular photo-treatments, the hydrophobic photosensitizers were still incorporated into the nanostructures in their aggregated form, presumably reducing their phototherapeutic capabilities. Thus, in order to maximize the synergistic effect of both

prevent its photodegradation even at relatively long laser irradiation times.⁹⁻¹¹ However, systemic administration with a minimal dose of the photosensitizer is still needed to avoid potential side effects.¹²⁻¹⁴

^aDepartment of Bio and Brain Engineering, and Institute for Optical Science and Technology, Korea Advanced Institute of Science and Technology, 291 Daehak-ro, Yuseong-gu, Daejeon 305-701, Korea. E-mail: jihopark@kaist.ac.kr

^bInstitute for the Nanocentury, Korea Advanced Institute of Science and Technology, Daejeon 305-701, Korea

[†] Electronic supplementary information (ESI) available. See DOI: 10.1039/c3tb21452d

 $[\]ddagger$ These authors contributed equally to this work.

PDT and PTT, new formulations of photoactive nanostructures that allow for the incorporation of hydrophobic photosensitizers in their monomeric form and the use of a single laser need to be developed.

Herein, we present plasmonic liposomes (PLs), which can be activated using a single laser, enabling synergistic photodynamic and photothermal therapy (Fig. 1). The PLs were prepared by incorporating ZnPc into the liposomal membrane for PDT and coating a gold nanofilm onto the surface for PTT. The gold coating was optimized to efficiently absorb the wavelength of light at which ZnPc is activated for PDT. A single 660 nm excitation wavelength was used to activate both the PD and PT functions of ZnPc-loaded PLs (ZnPc-PLs) simultaneously. Due to the synergistic effect of the dual phototherapy, ZnPc-PLs exhibited a remarkably enhanced therapeutic efficacy on cancer cells in vitro, compared to PDT or PTT alone. These results demonstrate that ZnPc-PLs can serve as a biocompatible nano-platform for effective dual phototherapy by bridging the gap between PDT and PTT without the use of complicated multiple laser sources.

2. **Experimental section**

2.1. Preparation of ZnPc-loaded liposomes

Hydrogenated soy sn-glycero-3-phosphocholine (HSPC), cholesterol, and 1,2-dipalmitoyl-sn-glycero-3-phosphoethanolamine-N (hexanoylamine) (PE-NH2) were purchased from Avanti Polar Lipids (Alabaster, AL). Zinc phthalocyanine (ZnPc) was purchased from Sigma Chemical Co. (St. Louis, MO). Aminated liposomes were prepared from HSPC, cholesterol, and PE-NH2 at a molar ratio of 69:50:6 using a lipid film hydration and membrane (100 nm) extrusion method. Aminated ZnPc-loaded liposomes (ZnPc-Ls) were prepared with HSPC, ZnPc, and PE-NH₂ at a molar ratio of 69:2:6 using a lipid film hydration and membrane (100 nm) extrusion method. The prepared liposomes were stored in PBS at 4 °C before use. The liposomes were characterized via transmission electron microscopy (TEM) and dynamic light scattering (DLS). For the TEM imaging, an aliquot of liposomes dispersed in water was dropped onto the formvar/ carbon grid (Ted Pella, Inc., CA, USA), which was then gently wiped off after approximately 1 min and air-dried. For negative

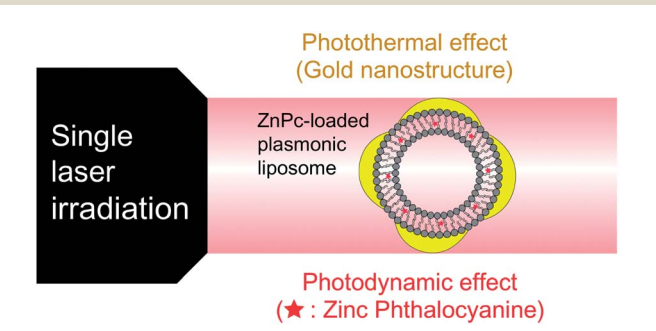


Fig. 1 A schematic illustration of the ZnPc-loaded plasmonic liposomes prepared for synergistic photodynamic and photothermal therapy upon single irradiation. Both the gold nanostructure and ZnPc are activated by absorbing light of the same wavelength.

staining, the grid was incubated with 2% phosphotungstic acid at pH 8 for an additional 1 min. TEM images were obtained using a JEM-2100F HRTEM operating at 200 kV. For the DLS measurements, the hydrodynamic size and polydispersity of the samples (~5 μM ZnPc) were obtained using a Zetasizer ZS90 DLS machine operating in intensity mode using a 640 nm HeNe laser (Malvern Instruments, Worcestershire, UK). The optical properties were analyzed using a SpectraMax Plus384 absorbance microplate reader and a Gemini XPS fluorescence microplate reader (Molecular Devices, CA, USA). In order to obtain the entrapping efficiency and actual loading concentration of ZnPc in ZnPc-L, the absorbance of ZnPc in ZnPc-Ls was compared to that of free ZnPc (dissolved in pyridine) at various concentrations. In order to verify the loading stability of ZnPc in the liposomes in biological media, ZnPc-Ls were incubated for 6 h in a cell culture medium at 37 °C. Time-dependent absorption spectra of ZnPc-Ls were measured during the 6 h incubation period.

2.2. Preparation of the ZnPc-loaded plasmonic liposomes

First, a gold ion solution was prepared using 2.4 ml of DI water, 0.3 ml of 1% HAuCl₄·3H₂O, and 36 μl of 1 N NaOH. The mixture was aged for more than 1 h at room temperature. The plasmonic liposomes (PLs) were prepared by coating the aminated liposomes or ZnPc-Ls with a gold nanofilm using previously established deposition-precipitation (DP) protocol.34 In order to control the thickness of the gold coating on the PLs, the aminated liposomes were reacted with different amounts of gold ion solution. The PLs are classified by the relative amount of gold ion solution mixed with the liposomes; PL-1, PL-2, PL-4, and PL-10 i.e. 100 µl of aminated liposomes were reacted with 90 μl of gold ion solution and 810 μl of DI water (PL-1); 180 μl of gold ion solution and 720 μl of DI water (PL-2); 360 μl of gold ion solution and 540 μl of DI water (PL-4); or only 900 µl of gold ion solution (PL-10). After incubation for 10 min, 140 μl of 20 mM NH₂OH·HCl was added to the reaction solution as a reductant. The solution was centrifuged at 7000 rpm for 10 min to remove any uncoated liposomes. For PEGylation, ZnPc-PLs were mixed with 5 kDa methyl-PEG-thiol (Laysan Bio, Inc.) at room temperature for 1 h, and dialyzed exhaustively against DI water via cellulose ester membrane dialysis overnight in order to drive PEG addition (Spectrapor). The dialyzed samples were filtered through 100 kDa filters (Millipore) to remove any excess polymer. The size and morphology of PLs were characterized using DLS and TEM. Optical properties of PLs and ZnPc-PLs were measured using a SpectraMax Plus384 absorbance microplate reader and a Gemini XPS fluorescence microplate reader. For the fluorescence measurements, the samples were excited at 610 nm. In order to quantify the amount of ZnPc in the ZnPc-PLs, ZnPc-PLs were centrifuged at 7000 rpm for 10 min and the absorbance of ZnPc in the supernatant (uncoated ZnPc-Ls) was measured giving the amount of ZnPc in the uncoated ZnPc-Ls. Finally, the amount of ZnPc in the ZnPc-PLs was obtained by subtracting the amount of ZnPc in the uncoated ZnPc-Ls from the amount of ZnPc in the reacted ZnPc-Ls.

2.3. Measurement of the photothermal and photodynamic effect

The photothermal and photodynamic properties of the samples were simultaneously evaluated using a single laser source. 380 µl of each sample was placed in a 96-well plate, and 5 μl of singlet oxygen sensor green (3.3 μM SOSG, Invitrogen, CA, USA) was added, which emits a green fluorescence in the presence of singlet oxygen (Fig. S4†). Each sample was exposed to a 660 nm diode laser (0.18 W cm⁻², Sanctity Laser) for 5 min. The photothermal effect was analyzed in real-time using an IR thermographic camera (FLIR SC305, CA, USA). The photodynamic effect was analyzed by removing ZnPc-PLs from the sample by centrifugation, and performing a SOSG fluorescence measurement of the samples. In order to verify the photostability of ZnPc incorporated in the ZnPc-Ls in biological media, the photodynamic effect of ZnPc-Ls incubated in the culture medium over each period of time were measured using the SOSG fluorescence sensor. In order to observe whether the photodynamic effect would be enhanced with a temperature increase, ZnPc-Ls samples were heated to 37 °C and 45 °C in a temperature-controlled water bath and then irradiated with a 660 nm laser for 5 min. The photodynamic effect was analyzed by measuring the green fluorescence of the samples.

2.4. In vitro dual phototherapy

A mouse colon cancer cell line (CT-26), a human breast cancer cell line (MDA-MB-231) and a mouse brain endothelial cell line were maintained in a culture media supplemented with 10% fetal bovine serum (FBS) and 100 μg ml⁻¹ penicillin-streptomycin (Hyclone) at 37 °C. For cell uptake, the cells (20k cells per well) were seeded into a 96-well plate 24 h before the experiments. The cells were treated with ZnPc-PLs with different concentrations of ZnPc (0 μM, 0.0275 μM, 0.275 μM, or 2.75 μM) per well for 4 h at 37 °C in the presence of 10% FBS, and then rinsed three times with the cell medium. The cells were then stained with Hoechst, a blue fluorescent indicator for nucleic acids (Invitrogen), or calcein AM, a green fluorescent indicator of the esterase activity in viable cells, (Invitrogen) in order to visualize the cellular morphology and evaluate the cytotoxicity. The cells were imaged using confocal fluorescence microscopy. ZnPc fluorescence in the ZnPc-PLs was observed in the far-red channel, while calcein fluorescence was observed in the FITC channel (excitation at 490 nm/emission at 520 nm). For the dual phototherapeutic studies, the cells were treated either with various ZnPc-loaded liposomal formulations at a ZnPc concentration of 0.275 µM or control formulations for 4 h. The concentrations of the liposomes and PLs were adjusted to match the concentrations of the liposomes in the ZnPc-L (0.275 μ M ZnPc) sample and PLs in the ZnPc-PL (0.275 μ M ZnPc) sample, respectively. ZnPc-PL samples with various particle concentrations (0.275 µM, 0.550 µM, 1.1 µM and 2.75 μM ZnPc) were also tested for their dual therapeutic efficacy. The cells were incubated with each ZnPc-PL sample for 4 h and then irradiated under a 660 nm laser for 5 min. The treated cells were rinsed three times and incubated for 24 h. Their viability

was then evaluated using an MTT assay. A Student's *t*-test was used for statistical analysis of the results.

3. Results and discussion

PLs were prepared by coating a gold nano-film on the liposomal surface using a previously established deposition-precipitation protocol with some slight modifications.34 Positively-charged liposomes between 90-110 nm in size (polydispersity index: 0.245 ± 0.022) were chosen as templates for gold coating (Fig. S1†). The thickness of the gold coating was tuned by varying the amount of gold ions in the reaction solution. Relative gold ion concentrations from 1 to 10 are referred to in the samples labeled PL-1 to PL-10. The optical spectra of PLs were changed by varying the thickness of the gold coating and were found to be relatively sharp in the visible to NIR range compared to previous versions of the gold-coated liposomes, which had a similar range of sizes (Fig. S2†).35,36 As the thickness increased, the spectrum shifted to shorter wavelengths, which is in good agreement with the previous findings on gold nanoshells.37 Gold nanoparticles synthesized without liposome templates appeared spherical with sizes ranging between 50 and 70 nm, and exhibited the typical plasmonic spectrum of gold nanospheres at a wavelength of 530 nm (Fig. S3†). The PL-4 formulation was chosen for the incorporation of ZnPc molecules because its plasmonic resonance wavelength for PTT matched well with the absorption wavelength at which ZnPc is excited for PDT.

In order to integrate both PD and PT functions into a single nanodevice, we prepared ZnPc-PLs by loading ZnPc molecules into the liposomal membrane and subsequently coating the ZnPc-loaded liposomes (ZnPc-Ls) with a gold layer using the coating conditions used to prepare PL-4. The efficiency of entrapping ZnPc into the liposomes was 25.073 \pm 2.131% (ZnPc concentration: 16.104 \pm 1.419 μ M). The ZnPc incorporated into the liposomal membrane was not significantly released and aggregated in the biological medium over an incubation period of 6 h, indicating good stability of the incorporated ZnPc (Fig. S4†). From transmission electron microscopy (TEM), the ZnPc-PLs appeared fairly spherical with discontinuous gold coatings and sizes in the range of 70-100 nm (Fig. 2a). The mean hydrodynamic size measured using dynamic light scattering (DLS) was about 85 nm, which is consistent with the TEM measurements. ZnPc-PLs showed a distinct absorption peak at 680 nm, which matched well with the excitation wavelength of ZnPc for PDT (Fig. 2b and c). Although the absorption spectrum of the loaded ZnPc was overwhelmed by that of the PLs, its fluorescence peak was clearly observed within the ZnPc-PL sample (Fig. 2d). The relatively low fluorescence intensity of ZnPc loaded into the PLs in comparison with that of ZnPc loaded in the liposomes can be attributed to partial quenching of the ZnPc fluorescence by gold nanostructures adjacent to the ZnPc molecules. Finally, the as-synthesized ZnPc-PLs were well dispersed in an aqueous solution. PEGylation of the ZnPc-PLs enabled their prolonged solubility in a physiological solution.

Next, the photothermal and photosensitizing properties of ZnPc-PLs were simultaneously evaluated using a single

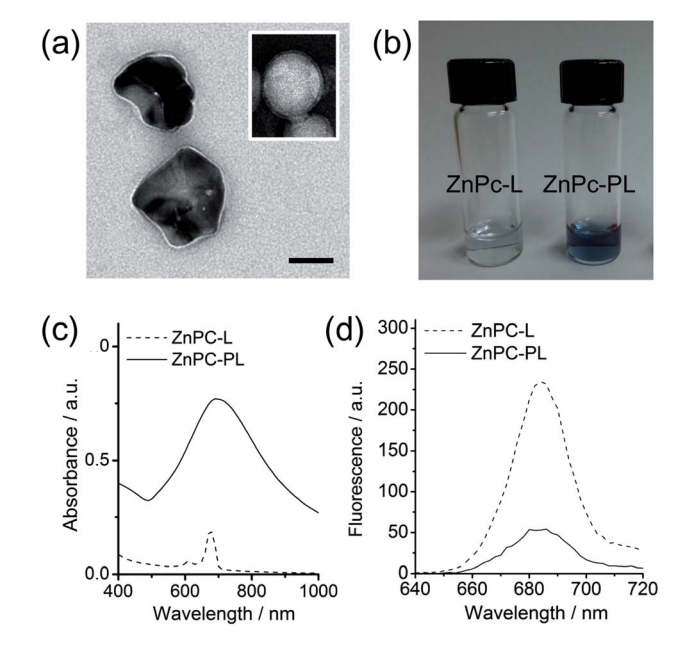


Fig. 2 Physical and optical properties of the ZnPc-loaded plasmonic liposomes (ZnPc-PLs). (a) Transmission electron microscopy image of ZnPc-PLs [inset: TEM image of the ZnPc-loaded liposomes (ZnPc-Ls) with negative staining by 2% phosphotungstic acid at pH 8]. The scale bar indicates 50 nm. (b) Photograph of ZnPc-PLs and ZnPc-Ls. (c) Absorption spectra of ZnPc-Ls and ZnPc-PLs. (d) Fluorescence spectra of ZnPc-Ls and ZnPc-PLs. The nanoparticle samples were excited with 610 nm light

continuous-wave diode laser (660 nm, 0.18 W cm⁻²) (Fig. S5†). Various ZnPc-PL and ZnPc-L samples were prepared based on different concentrations of loaded ZnPc (0.01 µM, 0.1 µM, 1 µM and 10 μ M). The concentrations of the liposome and PL samples were adjusted to match the concentrations of the liposomes in the ZnPc-L (10 µM ZnPc) sample and PLs in the ZnPc-PL (10 µM ZnPc) sample, respectively. The photothermal effect in the samples was measured in real-time using an IR thermographic camera. Upon 660 nm laser irradiation, the ZnPc-PLs at the highest concentration (10 µM ZnPc) exhibited a temperature increase of 20 °C (Fig. 3a). The PT effect of ZnPc-PLs is similar to that of PLs alone, suggesting that the incorporation of ZnPc into the liposomal membrane did not influence the coating of the gold nanostructure onto the liposomal template. The photothermal heating of ZnPc-PLs increased with increasing particle concentration. The liposomes alone and ZnPc-Ls did not show significant temperature increases. Thus, the PT effect of ZnPc-PLs can mainly be attributed to the gold nanostructure coated on the liposome surface, which efficiently converts the absorbed light into heat.

The PD effect of the samples was analyzed with the singlet oxygen sensor green (SOSG) fluorescent sensor in order to measure the level of singlet oxygen generation. Sample solutions mixed with SOSG were exposed to laser irradiation. The SOSG fluorescence of the ZnPc-L and ZnPc-PL samples increased with increasing particle concentration (Fig. 3b). Notably, the photosensitizing effect of ZnPc-PLs with a ZnPc concentration of 1 µM was significantly enhanced compared to

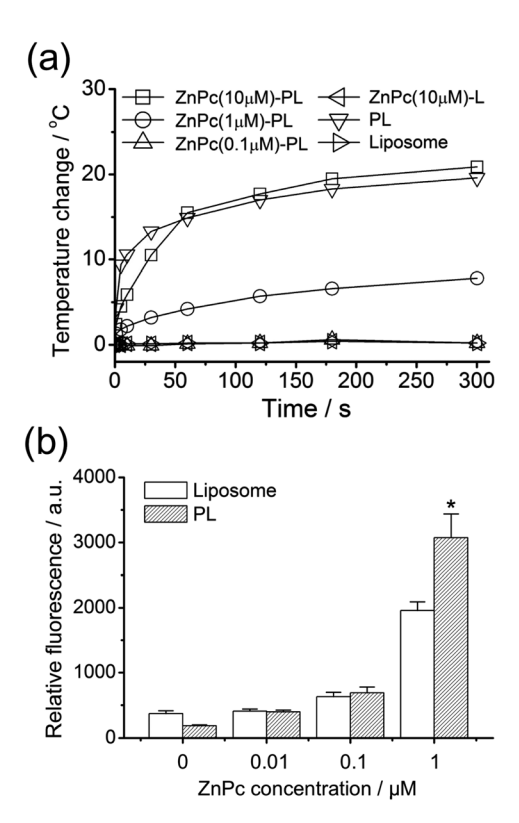


Fig. 3 Photothermal and photodynamic effect of ZnPc-loaded plasmonic liposomes (ZnPc-PLs). (a) Photothermal effect of samples upon 660 nm laser irradiation. The temperature change of the samples was measured in real-time using an IR thermographic camera. ZnPc-PL and ZnPc-loaded liposomes (ZnPc-Ls) with different concentrations were prepared based on the concentration of loaded ZnPc (0.1 μM, 1 μM and 10 μM). The concentrations of the liposomes and PLs were adjusted to match with the concentration of liposomes in the ZnPc-L (10 μ M ZnPc) sample and with the concentration of PLs in the ZnPc-PL (10 μM ZnPc) sample, respectively. (b) The photodynamic effect of the samples upon 660 nm laser irradiation. ROS generated in the samples was measured with a SOSG fluorescent sensor. The values are means \pm s.d. * p < 0.05 compared to ZnPc-L (1 μ M ZnPc) using an independent-samples t-test.

that of ZnPc-Ls with the same concentration of ZnPc. The discontinuous coating of the gold layer shown in the TEM image (Fig. 2a) seems to enable the transport of singlet oxygen generated by the incorporated ZnPc to the surroundings. It is believed that local photothermal heating and the surface plasmon resonance (SPR) of the gold nanostructure of ZnPc-PLs upon light irradiation leads to a dramatic enhancement of the photosensitizing effect.38,39 It should be noted that ZnPc-PLs with a ZnPc concentration of 1 µM did not induce sufficient heating to cause undesirable damage to the surrounding normal tissues upon light irradiation (an increase of only about 5 °C). Next, we measured the SOSG fluorescence in the ZnPc-L (1 μM ZnPc) sample at 20, 37, and 45 °C in order to test whether local heating could indeed influence the photosensitizing effect of ZnPc. The sensor fluorescence increased with increasing temperature, supporting the idea that local heating could be one of the factors amplifying the PD efficacy of ZnPc-PLs (Fig. S6†), which is consistent with previous findings. 40

Therefore, these results suggest that ZnPc–PLs could be used to perform synergistic dual phototherapy using an appropriate range of particle concentrations.

In order to test their phototherapeutic effect on cancer cells in vitro, we first verified whether ZnPc–PLs could be safely translocated into intracellular regions. CT26 mouse colon carcinoma cells were treated with ZnPc–PLs with various particle concentrations for 4 h and imaged using confocal microscopy (Fig. 4a–d). After treatment, the intrinsic fluorescence of ZnPc loaded into the PLs was clearly observed in the intercellular region of the samples at higher concentrations (0.275 μM and 2.75 μM ZnPc), indicating that the ZnPc–PLs were indeed internalized into the cytoplasm within the tested time period. The cells were further stained with calcein AM, which fluoresces green in viable cells (Fig. S7†). The cells treated with ZnPc–PL samples exhibited strong green fluorescence over the entire cytoplasm regardless of the treated particle

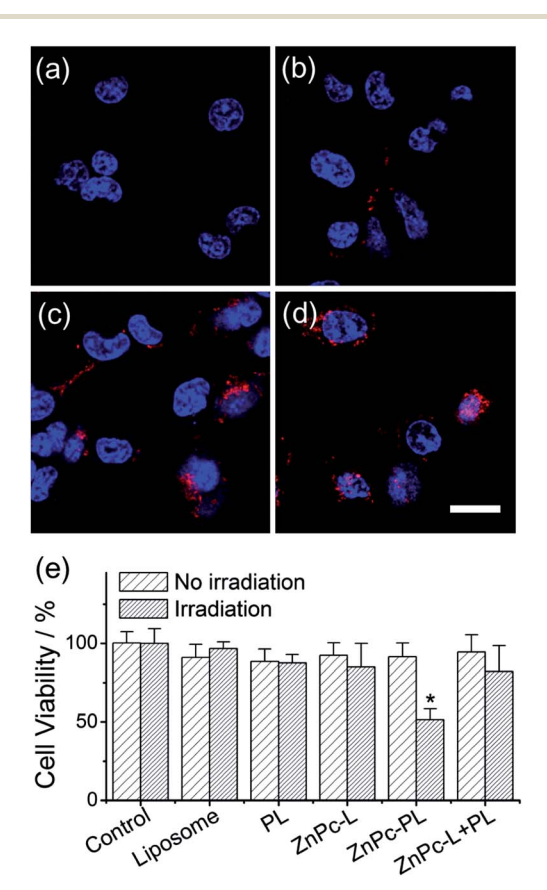


Fig. 4 The synergistic phototherapeutic effect of ZnPc-loaded plasmonic liposomes (ZnPc-PLs). Confocal microscopy images of cancer cells treated with ZnPc-PLs with concentrations of (a) 0 μ M ZnPc, (b) 0.0275 μ M ZnPc, (c) 0.275 μ M ZnPc, and (d) 2.75 μ M ZnPc. The red signal represents the ZnPc loaded into the ZnPc-PLs and the blue signal represents the cell nuclei. The scale bar indicates 30 μ m. (e) The dual phototherapy efficacy of ZnPc-PLs with a ZnPc concentration of 0.275 μ M on cancer cells upon 660 nm laser irradiation for 5 min. The cell viability was measured using an MTT assay 24 h after treating the cells with the various nanoparticle samples and light irradiation. Values are means \pm s.d. * p < 0.05 compared to ZnPc-PL without irradiation, PL with irradiation, ZnPc-L with irradiation, and ZnPc-L + PL with irradiation using an independent-samples t-test.

concentration, indicating that the intracellular uptake of ZnPc–PL nanomaterials did not induce any significant cytotoxicity. ZnPc–PLs at the medium concentration (0.275 μ M ZnPc) were chosen for the subsequent *in vitro* synergistic phototherapeutic studies .

After establishing the safe intracellular delivery of ZnPc-PLs, we evaluated the dual phototherapeutic efficacy of ZnPc-PLs internalized in the cytoplasm. ZnPc-L and ZnPc-PL samples were prepared based on the concentration of loaded ZnPc (0.275 µM). The concentrations of the liposome and PL samples were adjusted to match the concentrations of the liposomes in the ZnPc-L (0.275 µM ZnPc) sample and PLs in the ZnPc-PL (0.275 μM ZnPc) sample, respectively. The ZnPc-L + PL sample was prepared by mixing ZnPc-Ls and PLs at equivalent concentrations of ZnPc, liposomes and PLs. The cancer cells were treated with the various nanoparticle formulations for 4 h, and half of the cells were irradiated using a 660 nm laser. At 24 h post-treatment, the phototoxicity of the samples was analyzed using a 3-(4,5-dimethylthiazol-2-yl)-2,5-diphenyltetrazolium bromide (MTT) assay (Fig. 4e). None of the samples induced significant cytotoxicity in the cancer cells without laser irradiation. The cells treated with the liposome sample did not exhibit any phototoxicity under laser irradiation, indicating that the light itself did not damage the cancer cells. Neither the cells treated with PLs nor ZnPc-Ls exhibited a significant reduction in the cell viability upon laser irradiation. This suggests that singular phototherapy with PLs or ZnPc-Ls at this particular particle concentration is not sufficient enough to kill the cancer cells. Most importantly, the ZnPc-PL sample induced significant cellular phototoxicity, presumably owing to the synergistic dual phototherapeutic effect. This dual phototherapeutic efficacy of ZnPc-PLs increased with increasing particle concentration (Fig. S8†). However, the mixture of PLs and ZnPc-Ls did not exhibit a significant phototherapeutic effect on the cancer cells, indicating that the ZnPc molecules are required to be adjacent to the gold nanostructure in order to enhance their photodynamic effect. The synergistic phototherapeutic effect of ZnPc-PLs was also observed in human breast cancer cells (Fig. S9†). Interestingly, no therapeutic effect was found in normal endothelial cells, presumably due to their low uptake of liposomes (Fig. S10†). Collectively, these results suggest that ZnPc-PLs internalized in the cytoplasm could effectively kill the cancer cells due to the synergistic therapeutic effect upon laser irradiation.

4. Conclusions

PLs were developed to carry hydrophobic photosensitizers and perform dual phototherapy using a single light source. The results of this study demonstrated, for the first time, that the photosensitizing effect of ZnPc loaded in PLs could be dramatically enhanced when combined with SPR and the photothermal heating of the gold nanostructures in the PLs upon laser irradiation. A major advantage of these multi-modal nanodevices is that a large synergistic effect can be achieved with a much lower dosage, at which single-modal nanodevices have no therapeutic efficacy. The PLs also allow for the

incorporation of hydrophilic anti-cancer drugs into their liposomal core, thus further increasing the synergistic potential of this combined therapy. Therefore, we believe that this dual photoactive nanodevice with a synergistic therapeutic index has great potential to improve the current phototherapy of cancer.

Acknowledgements

Paper

This work was supported by the National R&D Program for Cancer Control, Ministry for Health and Welfare, Republic of Korea (grant no. 1220070). The authors thank Dr Pilhan Kim and Howon Seo of KAIST for assistance with confocal microscopy and Dr Seok Hyun Yun and Yirang Kim of KAIST for kindly providing the laser facility.

Notes and references

- 1 T. J. Dougherty, C. J. Gomer, G. Jori, D. Kessel, M. Korbelik, J. Moan and Q. Peng, J. Natl. Cancer Inst., 1998, 90, 889–905.
- 2 Y. N. Konan, R. Gurny and E. Allémann, J. Photochem. Photobiol., B, 2002, 66, 89-106.
- 3 X. Huang, P. Jain, I. El-Sayed and M. El-Sayed, *Lasers Med. Sci.*, 2008, 23, 217–228.
- 4 J. W. Owens, R. Smith, R. Robinson and M. Robins, *Inorg. Chim. Acta*, 1998, **279**, 226–231.
- 5 W. S. Chan, N. Brasseur, G. L. Madeleine, R. Quellet and J. E. van Lier, *Eur. J. Cancer*, 1997, 33, 1855–1859.
- 6 E. Reddi, C. Zhou, R. Biolo, E. Menegaldo and G. Jori, *Br. J. Cancer*, 1990, **61**, 407–411.
- 7 M. N. Sibata, A. C. Tedesco and J. M. Marchetti, *Eur. J. Pharm. Sci.*, 2004, 23, 131–138.
- 8 E. Ricci-Júnior and J. M. Marchetti, *Int. J. Pharm.*, 2006, **310**, 187–195.
- 9 A. M. Garcia, E. Alarcon, M. Munoz, J. C. Scaiano, A. M. Edwards and E. Lissi, *Photochem. Photobiol. Sci.*, 2011, **10**, 507–514.
- 10 X. Damoiseau, H. J. Schuitmaker, J. W. M. Lagerberg and M. Hoebeke, *J. Photochem. Photobiol.*, *B*, 2001, **60**, 50–60.
- 11 S. Dhami and D. Phillips, *J. Photochem. Photobiol.*, *A*, 1996, **100**, 77–84.
- 12 E. I. Yslas, V. Rivarola and E. N. Durantini, *Bioorg. Med. Chem.*, 2005, **13**, 39–46.
- 13 W. Liu, N. Chen, H. Jin, J. Huang, J. Wei, J. Bao, C. Li, Y. Liu, X. Li and A. Wang, *Regul. Toxicol. Pharmacol.*, 2007, 47, 221–231.
- 14 H. Liu, D. Chen, L. Li, T. Liu, L. Tan, X. Wu and F. Tang, *Angew. Chem., Int. Ed.*, 2011, **50**, 891–895.
- 15 L. Au, J. Chen, L. Wang and Y. Xia, in *Cancer Nanotechnology*, ed. S. R. Grobmyer and B. M. Moudgil, Humana Press, 2010, vol. 624, pp. 83–99.
- 16 L. R. Hirsch, R. J. Stafford, J. A. Bankson, S. R. Sershen, B. Rivera, R. E. Price, J. D. Hazle, N. J. Halas and J. L. West, *Proc. Natl. Acad. Sci. U. S. A.*, 2003, **100**, 13549–13554.
- 17 G. von Maltzahn, J.-H. Park, A. Agrawal, N. K. Bandaru, S. K. Das, M. J. Sailor and S. N. Bhatia, *Cancer Res.*, 2009, 69, 3892–3900.

- 18 M. Zhang, T. Murakami, K. Ajima, K. Tsuchida, A. S. D. Sandanayaka, O. Ito, S. Iijima and M. Yudasaka, *Proc. Natl. Acad. Sci. U. S. A.*, 2008, **105**, 14773–14778.
- 19 W.-S. Kuo, C.-N. Chang, Y.-T. Chang, M.-H. Yang, Y.-H. Chien, S.-J. Chen and C.-S. Yeh, *Angew. Chem., Int. Ed.*, 2010, 49, 2711–2715.
- 20 B. Khlebtsov, E. Panfilova, V. Khanadeev, O. Bibikova, G. Terentyuk, A. Ivanov, V. Rumyantseva, I. Shilov, A. Ryabova, V. Loshchenov and N. G. Khlebtsov, ACS Nano, 2011, 5, 7077–7089.
- 21 B. Jang, J.-Y. Park, C.-H. Tung, I.-H. Kim and Y. Choi, ACS Nano, 2011, 5, 1086–1094.
- 22 B. Tian, C. Wang, S. Zhang, L. Feng and Z. Liu, ACS Nano, 2011, 5, 7000–7009.
- 23 J. Wang, G. Zhu, M. You, E. Song, M. I. Shukoor, K. Zhang, M. B. Altman, Y. Chen, Z. Zhu, C. Z. Huang and W. Tan, *ACS Nano*, 2012, 6, 5070–5077.
- 24 T. Murakami, H. Nakatsuji, M. Inada, Y. Matoba, T. Umeyama, M. Tsujimoto, S. Isoda, M. Hashida and H. Imahori, J. Am. Chem. Soc., 2012, 134, 17862– 17865.
- 25 L. Gao, J. Fei, J. Zhao, H. Li, Y. Cui and J. Li, ACS Nano, 2012, 6, 8030–8040.
- 26 W.-S. Kuo, Y.-T. Chang, K.-C. Cho, K.-C. Chiu, C.-H. Lien, C.-S. Yeh and S.-J. Chen, *Biomaterials*, 2012, 33, 3270– 3278.
- 27 J. Lin, S. Wang, P. Huang, Z. Wang, S. Chen, G. Niu, W. Li, J. He, D. Cui, G. Lu, X. Chen and Z. Nie, *ACS Nano*, 2013, 7, 5320–5329.
- 28 J.-Y. Kim, W. I. Choi, M. Kim and G. Tae, *J. Controlled Release*, 2013, **171**, 113–121.
- 29 A. Sahu, W. I. Choi, J. H. Lee and G. Tae, *Biomaterials*, 2013, 34, 6239–6248.
- 30 S. Wang, P. Huang, L. Nie, R. Xing, D. Liu, Z. Wang, J. Lin, S. Chen, G. Niu, G. Lu and X. Chen, *Adv. Mater.*, 2013, 25, 3055–3061.
- 31 R. Chen, X. Wang, X. Yao, X. Zheng, J. Wang and X. Jiang, *Biomaterials*, 2013, 34, 8314–8322.
- 32 S. Shi, X. Zhu, Z. Zhao, W. Fang, M. Chen, Y. Huang and X. Chen, *J. Mater. Chem. B*, 2013, **1**, 1133–1141.
- 33 M. Trapani, A. Romeo, T. Parisi, M. T. Sciortino, S. Patane, V. Villari and A. Mazzaglia, RSC Adv., 2013, 3, 5607– 5614.
- 34 J. Y. Kah, N. Phonthammachai, R. Y. Wan, J. Song, T. White, S. Mhaisalkar, I. Ahmadb, C. Shepparda and M. Olivoc, *Gold Bull.*, 2008, 41, 23–36.
- 35 T. S. Troutman, J. K. Barton and M. Romanowski, *Adv. Mater.*, 2008, **20**, 2604–2608.
- 36 Y. Jin and X. Gao, J. Am. Chem. Soc., 2009, 131, 17774-17776.
- 37 S. J. Oldenburg, R. D. Averitt, S. L. Westcott and N. J. Halas, Chem. Phys. Lett., 1998, 288, 243–247.
- 38 Y. Zhang, K. Aslan, M. J. R. Previte and C. D. Geddes, *Proc. Natl. Acad. Sci. U. S. A.*, 2008, **105**, 1798–1802.
- 39 M. K. Khaing Oo, Y. Yang, Y. Hu, M. Gomez, H. Du and H. Wang, *ACS Nano*, 2012, **6**, 1939–1947.
- 40 V. Gottfried and S. Kimel, *J. Photochem. Photobiol.*, *B*, 1991, **8**, 419–430.